JOURNAL OF MATERIALS SCIENCE 31 (1996) 172–184

Crystal growth kinetics in $BaOAl_2O_32SiO_2$ and $SrOAl_2O_32SiO_2$ glasses

M. J. HYATT, N. P. BANSAL*
National Aeronautics and Space Administration, Lewis Research Center, Cleveland, OH 44135, USA

Crystallization kinetics of $BaOAl_2O_32SiO_2$ (BAS) and $SrOAl_2O_32SiO_2$ (SAS) glasses in bulk and powder forms have been studied by non-isothermal differential scanning calorimetry (DSC). The crystal growth activation energies were evaluated to be 473 and 451 kJ mol^{-1} for bulk samples and 560 and 534 kJ mol^{-1} for powder specimens in BAS and SAS glasses, respectively. Development of crystalline phases on thermal treatments of glasses at various temperatures has been followed by powder X-ray diffraction. Powder samples crystallized at lower temperatures than the bulk and the crystallization temperature was lower for SAS glass than BAS. Crystallization in both glasses appeared to be surface nucleated. The high temperature phase hexacelsian, $MAl_2Si_2O_8$ (M = Ba or Sr), crystallized first by nucleating preferentially on the glass surface. Also, monoclinic celsian does not nucleate directly in the glass, but is formed at higher temperatures from the transformation of the metastable hexagonal phase. In SAS the transformation to monoclinic celsian occurred rapidly after 1 h at 1100 °C. In contrast, in BAS this transformation is sluggish and difficult and did not go to completion even after 10 h heat treatment at 1400 °C. The crystal growth morphologies in the glasses have been observed by optical microscopy. Some of the physical properties of the two glasses are also reported.

1. Introduction

One of the primary objectives of NASA's High Temperature Engine Materials Program (HITEMP) is the development of ceramic–matrix composites for employment in the hot section components of advanced aeropropulsion systems of the future. Glass and glass ceramics having typically low elastic modulus allow true reinforcement with high modulus ceramic fibres. Therefore, part of the effort includes the development of refractory glass–ceramics as potential matrix materials for fibre-reinforced composites. Glass–ceramics of feldspar composition, $MOAl_2O_32SiO_2$ (M = Ba or Sr), having monoclinic celsian crystalline phase are being investigated [1, 2] because of their high melting point, low thermal expansion, good oxidation resistance, and high temperature phase stability for reinforcement with ceramic fibres having high elastic modulus and high strength.

Previous studies [3, 4] have shown that glasses having near stoichiometric celsian composition invariably crystallize to the high temperature, metastable, hexacelsian phase upon heating. Hexacelsian undergoes [5, 6] a reversible displacive transformation to an orthorhombic or pseudo-hexagonal structure at low temperature. The accompanying large volume change makes it undesirable as a structural material. The low-temperature monoclinic celsian phase is stable up to ~1590 °C in the barium aluminosilicate (BAS) system and up to the melting point in the strontium aluminosilicate (SAS) system. Also, the kinetics of hexacelsian to celsian phase transformation are reasonably fast in the SAS system [7] but very sluggish in BAS [8, 9].

The primary objective of this study was to determine the heat treatment conditions required for formation of only the thermodynamically stable monoclinic celsian phase in BAS and SAS glass–ceramic matrices. To achieve this, the present study focused on the investigation of the kinetics of crystallization of barium- and strontium aluminosilicate glasses having stoichiometric celsian compositions. Thermal treatments at various temperatures and times were used to study the development of crystalline phases in these glasses. Such information is of value for processing of fibre-reinforced celsian composites.

2. Experimental procedures

BAS and SAS glasses of feldspar compositions were melted at temperatures greater than 2000 °C in a continuous electric arc furnace with Mo electrodes using laboratory-grade $BaCO_3$, $SrCO_3$, Al_2O_3, and SiO_2.

*Author to whom correspondence should be addressed.

0022–2461

TABLE I Batch and analysed compositions of glasses

Component	BAS		SAS	
	Batch	Analysed	Batch	Analysed
BaO	40.8	39.5	–	0.86
SrO	–	–	37.2	33.7
Al_2O_3	27.2	28.7	28.8	31.5
SiO_2	32.0	31.3	34.0	33.8
Na_2O	–	0.2	–	0.12
MoO_3	–	0.01	–	0.01

Homogeneous, clear, and colourless glass flakes were produced by quenching the melt between water-cooled metallic rollers. Glass specimens in the form of bars and rods were also fabricated. The flakes were wet ground in an attrition mill using zirconia or alumina media, resulting in fine glass powders having an average particle diameter of ~ 2.5 μm. The batch and analysed glass compositions are given in Table I. The Ba, Sr, Al, and Si contents in the glasses were determined from wet chemical analysis and Mo by spectrographic technique. The estimated uncertainties of the two methods were $\pm 1\%$ and $\pm 10\%$, respectively. The source of trace amounts of MoO_3 in the glasses was the Mo electrodes used during electric melting.

Bulk glass samples for property measurements were annealed in an electric furnace for 1 h at 800 °C in air. Densities were measured by Archimedes' method using a Mettler AE200 electronic balance with a ME40290 density kit. Thermal expansion coefficient (α), glass transition temperature (T_g), and dilatometric softening temperature (T_s) were measured with a Perkin-Elmer TMA-7 thermomechanical analysis system.

Crystallization kinetics of the glasses were studied by non-isothermal differential scanning calorimetry (DSC) using a Stanton Redcroft DSC-1500 system interfaced with a computerized data acquisition and analysis system. Glass samples were contained in alumina or Pt cups. The crystallization peak maximum temperatures (T_p) of bulk and powder glasses were determined in flowing dry argon as a function of scan rate which varied from 2 to 40 °C min^{-1}. Glass transition temperatures were also obtained from the DSC and compared with the values measured by TMA.

The development of crystalline phases in the glasses was investigated by isothermal heat treatments of bulk and powder samples in air in an electric furnace. The samples were heat treated for 1 or 10 h at various temperatures from 950 to 1400 °C at 50 °C intervals. Phases crystallizing in the heat treated glasses were identified from powder X-ray diffraction (XRD) patterns recorded at room temperature using a step scan procedure (0.03°/2θ step, count time 0.4 s) on a Philips ADP-3600 automated diffractometer equipped with a crystal monochromator employing CuK_α radiation.

The morphologies of crystalline phases developed on heat treatment of bulk glass samples were examined by optical microscopy. Cross-sections of heat treated flakes were mounted perpendicular to their thickness in epoxy, ground, and polished to a 0.5 μm finish. The polished surfaces were given a light etch with HF.

3. Theoretical background

The crystallization kinetics of a glass at a constant temperature can be described by the Johnson–Mehl–Avrami (JMA) equation [10, 11]

$$-\ln(1-x) = (kt)^n \quad (1)$$

where x is the volume fraction of the glass crystallized after time t, n is the dimensionless Avrami exponent which is related to the morphology of crystal growth, and k is the reaction rate constant. The temperature dependence of k (at least within narrow temperature ranges) can be expressed by the Arrhenius equation

$$k = \nu \exp(-E/RT) \quad (2)$$

where ν is an effective frequency factor, E the effective overall activation energy, R the gas constant, and T the absolute reaction temperature.

During a non-isothermal DSC scan, the sample temperature changes linearly with time at a rate θ ($= dT/dt$)

$$T = T_i + \theta t \quad (3)$$

where T_i is the initial temperature. In Equation 1 the right-hand side corresponds to growth in volume of crystal nuclei. However, for the non-isothermal case the rate constant changes continuously with time due to the changing temperature, so that the JMA relation must be written as

$$-\ln(1-x) = [\int_0^t k(t)dt]^n \quad (4)$$

If at each temperature the deflection of the DSC trace from its baseline is proportional to the instantaneous crystallization rate (Borchard assumption [12]), then the rate of sample transformation is maximum at the peak of the crystallization exotherm. It has been shown by Bansal and colleagues [13, 14], the temperature T_p of the crystallization peak changes with heating rate θ according to the relation

$$\ln(T_p^2/\theta) = \ln(E/R\nu) + E/RT_p \quad (5)$$

Hence a plot of $\ln(T_p^2/\theta)$ versus $1/T_p$ should be linear with a slope of E/R and an intercept $[\ln(E/R) - \ln \nu]$. Equation 5 is based on the assumption that at a temperature corresponding to the maximum in the crystallization exothermic peak, the degree of crystallization attains the same specific value independent of the heating rate. Also, it may be pointed out that Equation 5 is applicable [14] only for the case where the crystal growth occurs from a fixed number of nuclei and is not useful when the number of crystal nuclei changes with the heating rate. Earlier studies [14–16] have shown that the crystallization kinetic parameters obtained by isothermal and non-isothermal DSC using Equation 5 are in good agreement.

Values of the Avrami parameter n can be evaluated from the non-isothermal data using an expression

derived by Piloyan *et al.* [17] and valid in the range $0 < x < 0.2$

$$d[\ln(\Delta y)]/d(1/T) = -nE/R \quad (6)$$

where (Δy) is the vertical displacement at temperature T of the DSC crystallization exotherm from the baseline. The Avrami parameter n gives an indication of the crystal growth mechanism in the glass.

4. Experimental results

4.1. Physical properties of glasses

Various physical properties of BAS and SAS glasses measured on unannealed samples, unless otherwise stated, are listed in Table II. Values of density, T_g, T_s, and crystallization onset temperatures, T_x, are greater for BAS than SAS glass. Both glasses have similar thermal expansion coefficients. The differences in physical properties of the two glasses may be attributed to the differences in chemistry of baria and strontia as components of the glass, though the similar values of thermal expansion coefficient of the two glasses is somewhat surprising. Higher values of T_g determined by DSC are probably due to the fact that unannealed specimens were used in these measurements. A knowledge of the properties of these glasses will be useful in establishing the processing parameters of fibre-reinforced glass–ceramic composites.

4.2. Crystallization kinetics by DSC

Typical DSC traces for bulk and powder samples of BAS and SAS glasses recorded at a heating rate of 40 °C min^{-1} are shown in Figs 1 and 2, respectively. The endotherm is due to the glass transition and the large exothermic peak at higher temperature is due to crystallization of the glass. The crystallization exotherm for the powder glasses is much sharper and occurs at a much lower temperature than the bulk sample. This probably indicates a surface nucleation, rather than a bulk nucleation, mechanism for crystallization of these glasses. Values of T_g and T_p determined from DSC at various scan rates from 2–40 K min^{-1} for bulk and powder BAS and SAS glasses are given in Tables III and IV, respectively.

TABLE II Physical properties of the glasses investigated

Property	Technique	BAS	SAS
ρ (g/cm^3)	Immersion	3.390 ± 0.04	3.040 ± 0.009
α (10^6/°C)[a, b]	TMA	6.4	6.3
T_g (°C)[b]	TMA	867	855
T_g (°C)[b]	DSC	885	871
T_s (°C)[b]	TMA	916	894
T_x (°C)[b, c] (Powder)	DSC	1017	1002
T_x (°C)[b, c] (Bulk)	DSC	1120	1075

[a] From 25 to 800 °C.
[b] 5 °C min^{-1} scan rate.
[c] Crystallization onset.

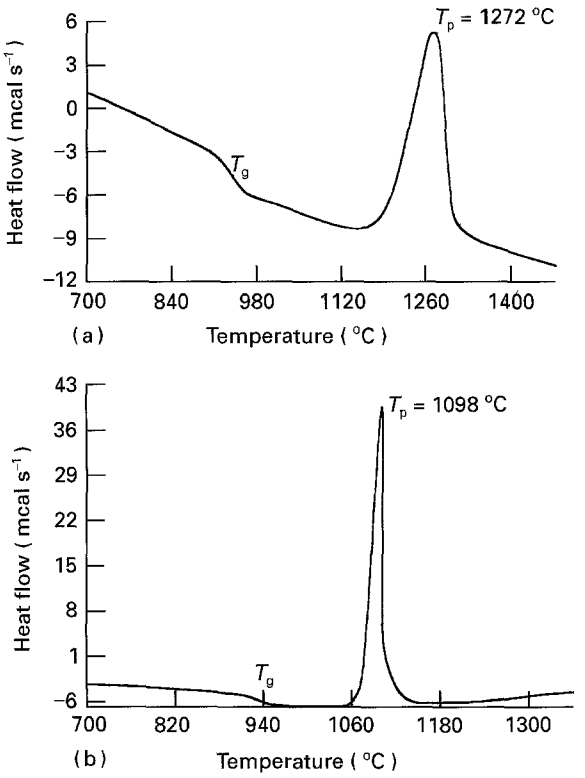

Figure 1 Comparison of DSC traces for (a) bulk and (b) powder samples of BAS glass recorded at a heating rate of 40 K min^{-1} under flowing argon.

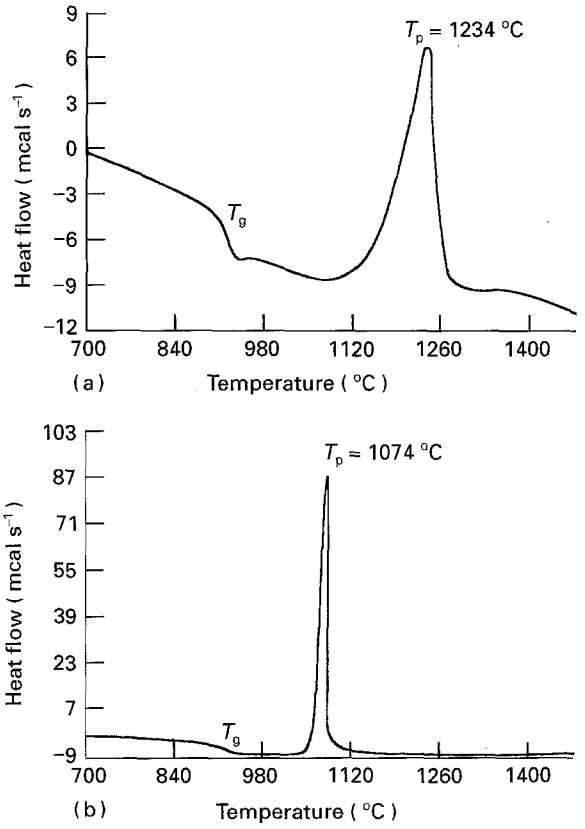

Figure 2 Non-isothermal DSC traces for (a) bulk and (b) powder samples of SAS glass at a heating rate of 40 K min^{-1} under flowing argon.

Plots of $\ln(T_p^2/\theta)$ versus $1/T_p$ (Equation 5) for crystallization of bulk and powder BAS and SAS glasses are presented in Fig. 3. Linear plots indicate

TABLE III Effect of scan rate on DSC glass transition (T_g) and crystallization peak maximum (T_p) temperatures for BAS glasses

Bulk glass			Powder glass		
Scan rate (°C min^{-1})	T_g (°C)	T_p (°C)	Scan rate (°C min^{-1})	T_g (°C)	T_p (°C)
2	–	1149	2	–	1020
5	885	1180	5	874	1038
10	890	1208	10	879	1053
10	895	1202	20	892	1071
20	902	1234	30	895	1086
20	902	1229	40	907	1098
30	909	1248			
30	906	1243			

TABLE IV Influence of scan rate on DSC glass transition (T_g) and crystallization peak maximum (T_p) temperatures for SAS glasses

Bulk glass			Powder glass		
Scan rate (°C min^{-1})	T_g (°C)	T_p (°C)	Scan rate (°C min^{-1})	T_g (°C)	T_p (°C)
2	–	1104	2	–	997
5	877	1140	5	870	1016
5	871	1137	10	880	1032
10	872	1166	20	884	1053
10	870	1162	30	892	1064
20	887	1185	40	895	1075
20	889	1181			
30	889	1204			
30	890	1203			
30	892	1202			

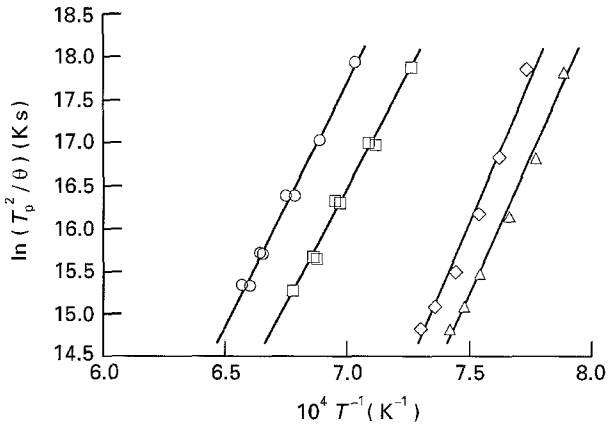

Figure 3 Plots of $\ln(T_p^2/\theta)$ versus reciprocal of crystallization peak maximum temperature for BAS and SAS glasses in bulk and powder forms. ○ BAS bulk; ◇ BAS powder; □ SAS bulk; △ SAS powder.

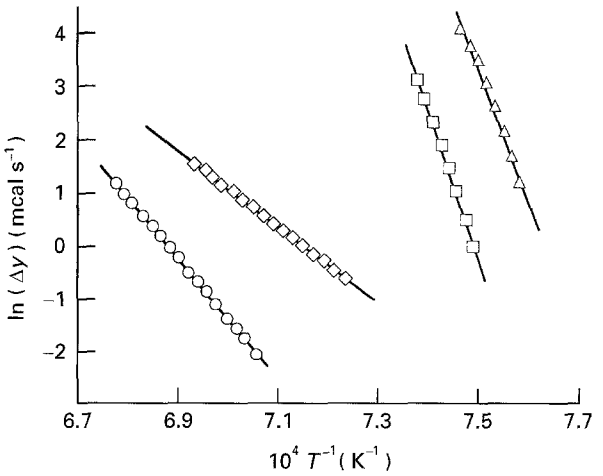

Figure 4 Piloyan plots for the crystallization of BAS and SAS glasses in bulk and powder forms for DSC thermograms recorded at a heating rate of 40 K min^{-1}. ○ BAS bulk; □ BAS powder; ◇ SAS bulk; △ SAS powder.

applicability of the kinetic model of Bansal *et al.* [13, 14] and validity of the assumptions made in this model. The Piloyan plots (Equation 6) of $\ln(\Delta y)$ versus $1/T$ for both BAS and SAS glasses, shown in Fig. 4, are also linear. Values of the crystallization kinetic parameters for the two glasses determined by linear least squares fitting of the experimental data to Equations 5 and 6 are given in Table V. Crystallization of SAS occurs with lower activation energy than BAS. In both glasses, a higher activation energy is found for powder than bulk samples. The value of n depends on the mechanism of the transformation reaction [14]. Values of n between 1 and 2 obtained for bulk glass would suggest one-dimensional growth of nuclei with a decreasing rate of nucleation. This would be plausible with a surface nucleated mechanism as indicated previously. Values of n near 4 found for powder samples indicates three-dimensional growth with constant or decreasing nucleation rate.

4.3. Crystal phase development by X-ray diffraction

The crystalline phases formed, as determined by powder XRD, on heat treatment of bulk and powder BAS and SAS glasses at various temperatures for 1 or 10 h, are summarized in Tables VI and VII. The phase listed first is the major phase present, based on relative intensities of XRD peaks. BAS glass crystallized at higher temperatures than SAS glass. In both glasses, powder samples crystallized and transformed to the monoclinic phase at lower temperatures and shorter

TABLE V Crystallization kinetic parameters for BAS and SAS glasses as determined by non-isothermal DSC

Glass	Activation energy, E (kJ mol^{-1})	Frequency factor, ν (s^{-1})	Avrami parameter (n)
BAS (bulk)	473	4.1×10^{13}	1.9 ± 0.1
BAS (powder)	560	9.0×10^{18}	3.8 ± 0.5
SAS (bulk)	451	2.2×10^{13}	1.4 ± 0.1
SAS (powder)	534	2.0×10^{18}	4.2 ± 0.4

TABLE VI Powder XRD results for development of crystalline phases in BAS and SAS glasses after 1 h heat treatment in air

Temperature (°C)	Bulk BAS	Bulk SAS	Powder BAS	Powder SAS
950	G	G, H(t)	G	G, H(t)
1000	G, H(t)	G, H	H	C, H
1050	G, H	H	H	C, H
1100	H, C(t)	H, C(t)	H, C	C
1150	H, C	H, C	H, C	C
1200	H, C	C, H	H, C	C
1250	H, C	C	H, C	C
1300	H, C	C	H, C	C
1350	H, C	C	H, C	C
1400	H, C	C	H, C	C

G Glass; H Hexacelsian; C Celsian; t trace.

TABLE VII Powder XRD results for development of crystalline phases in BAS and SAS glasses after 10 h heat treatment in air

Temperature (°C)	Bulk BAS	Bulk SAS	Powder BAS	Powder SAS
950	G, H(t)	G, H(t)	H	H, C
1000	H, G	H	H	C, H
1050	H	H, C(t)	H, C(t)	C
1100	H, C	H, C	H, C	C
1150	H, C	C	H, C	C
1200	H, C	C	H, C	C
1250	H, C	C	H, C	C
1300	H, C	C	H, C	C
1350	H, C	C	C, H	C
1400	H, C	C	C, H	C

G Glass; H Hexacelsian; C Celsian; t trace.

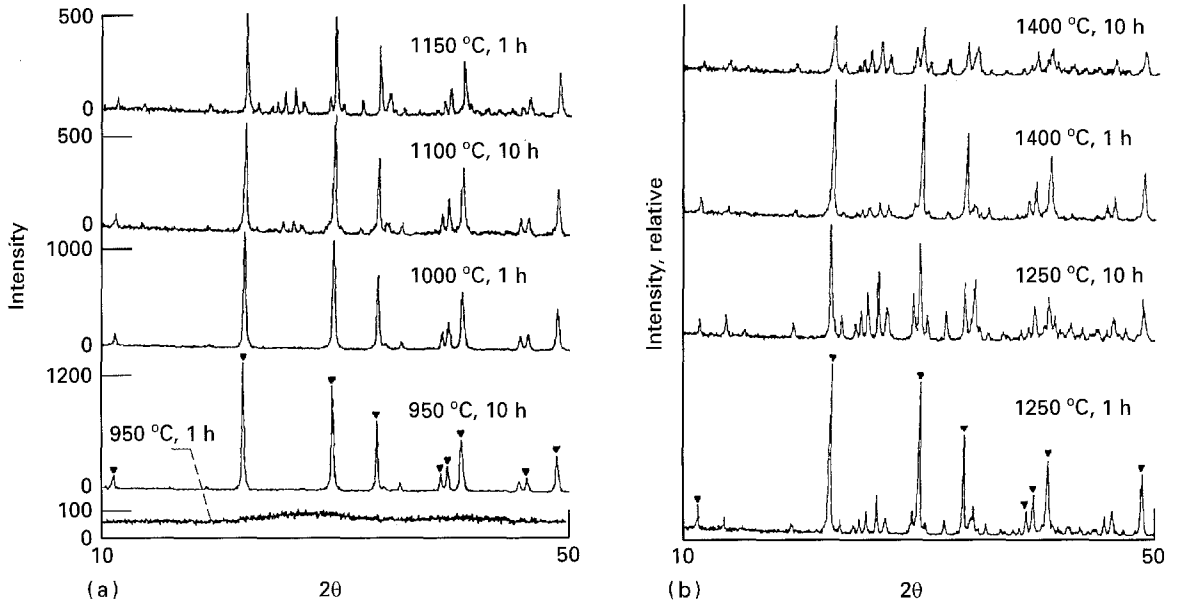

Figure 5 Powder X-ray diffraction patterns of BAS glass powder samples after heat treatments for 1 or 10 h at various temperatures. ▼ BAS hexagonal.

times than bulk samples. These results are in accordance with the DSC results (*vide supra*). BAS glass did not completely transform to the monoclinic celsian phase even after 10 h heat treatment at 1400 °C. On the other hand, SAS glass samples did completely transform to celsian rather easily – after 1 h at 1100 °C for powder and ~10 h at 1150 °C for bulk.

4.3.1. Powder glasses

Selected powder XRD patterns of BAS glass powder heat treated at various temperatures for 1 or 10 h are presented in Fig. 5. BAS remains amorphous after 1 h at 950 °C, but is completely crystallized to hexacelsian phase after 10 h at this temperature. Samples were also fully crystallized after 1 h heat treatment at 1000 °C.

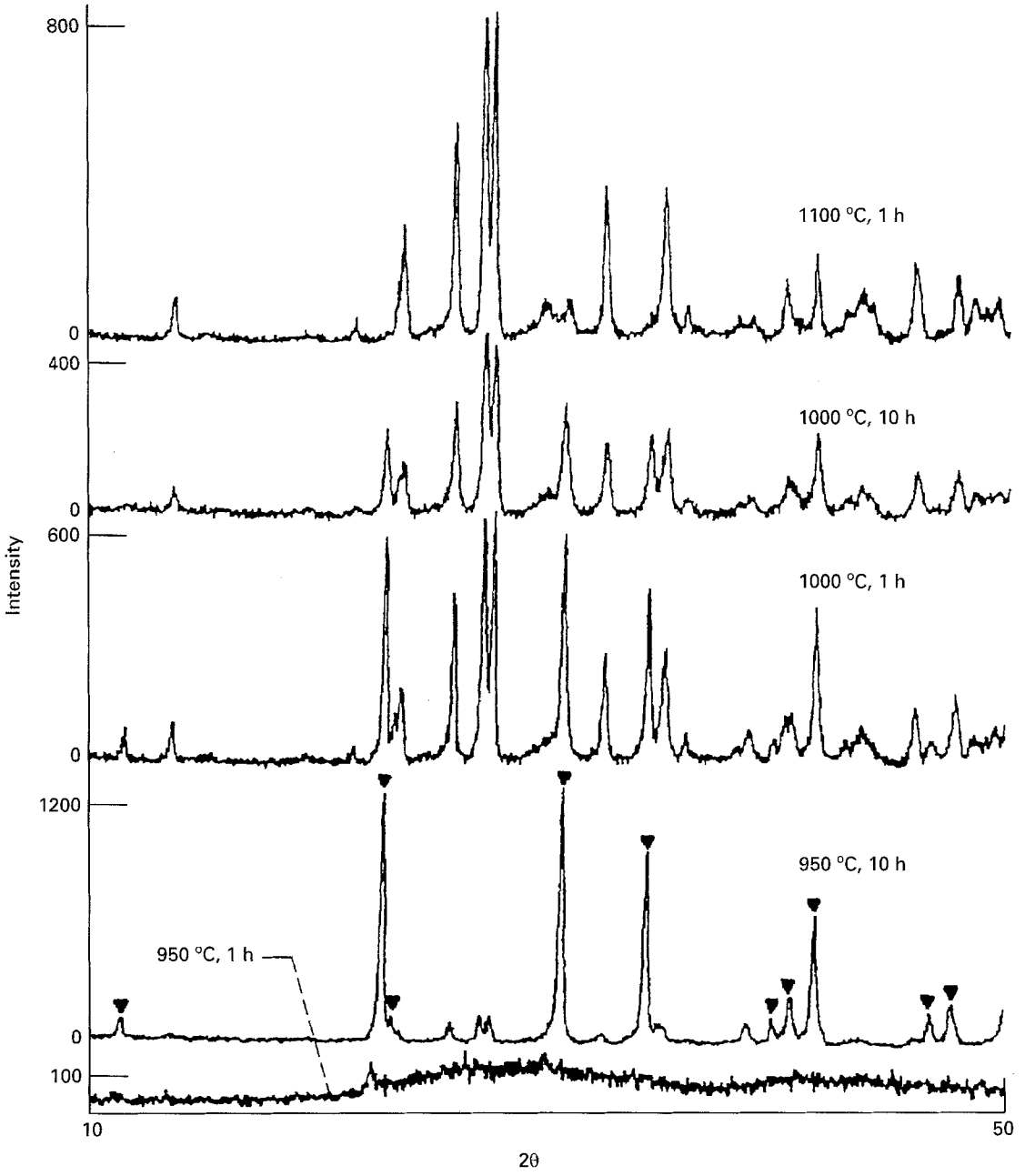

Figure 6 Powder X-ray diffractograms of SAS glass powder samples after thermal treatments for 1 or 10 h at various temperatures. ▼ SAS hexagonal.

The metastable hexacelsian phase begins to transform to the monoclinic celsian phase after 10 h at 1100 °C. The transformation occurs to a greater extent on 1 h heat treatment at 1150 °C. Fig. 5(b) shows the effect of time and temperature on the hexacelsian to celsian transformation in BAS glass powders. At 1250 and 1400 °C, a 1 h heat treatment produces a small amount of monoclinic phase. Even after 10 h heat treatment at 1400 °C, although the amount of monoclinic phase has increased relative to hexacelsian, the transformation is not yet complete. This illustrates the difficulty of attaining complete transformation to the monoclinic phase in BAS glass.

Selected powder XRD patterns of SAS glass powder samples heat treated at different temperatures for 1 or 10 h are presented in Fig. 6. Only a trace amount of hexacelsian phase is crystallized in the sample heat-treated for 1 h at 950 °C. On heat treatment for 10 h at 950 °C, the sample has completely crystallized and transformation of hexacelsian to celsian has also been initiated. The amount of celsian phase is considerably increased in the sample thermally treated for 1 or 10 h at 1000 °C. Only the monoclinic celsian phase is present after 10 h at 1050 °C or 1 h at 1100 °C.

4.3.2. Bulk glasses

The XRD results for BAS and SAS bulk glasses heat treated for 1 or 10 h are presented in Figs 7–10. Fig. 7 shows the powder XRD patterns for 1 h heat-treated bulk BAS glass samples at various temperatures. Crystallization is seen to initiate at 1000 °C and is completed at 1100 °C. The hexacelsian to monoclinic celsian transformation is detected at 1100 °C. Heat treatments at successively higher temperatures continue to increase the relative amounts of celsian, but

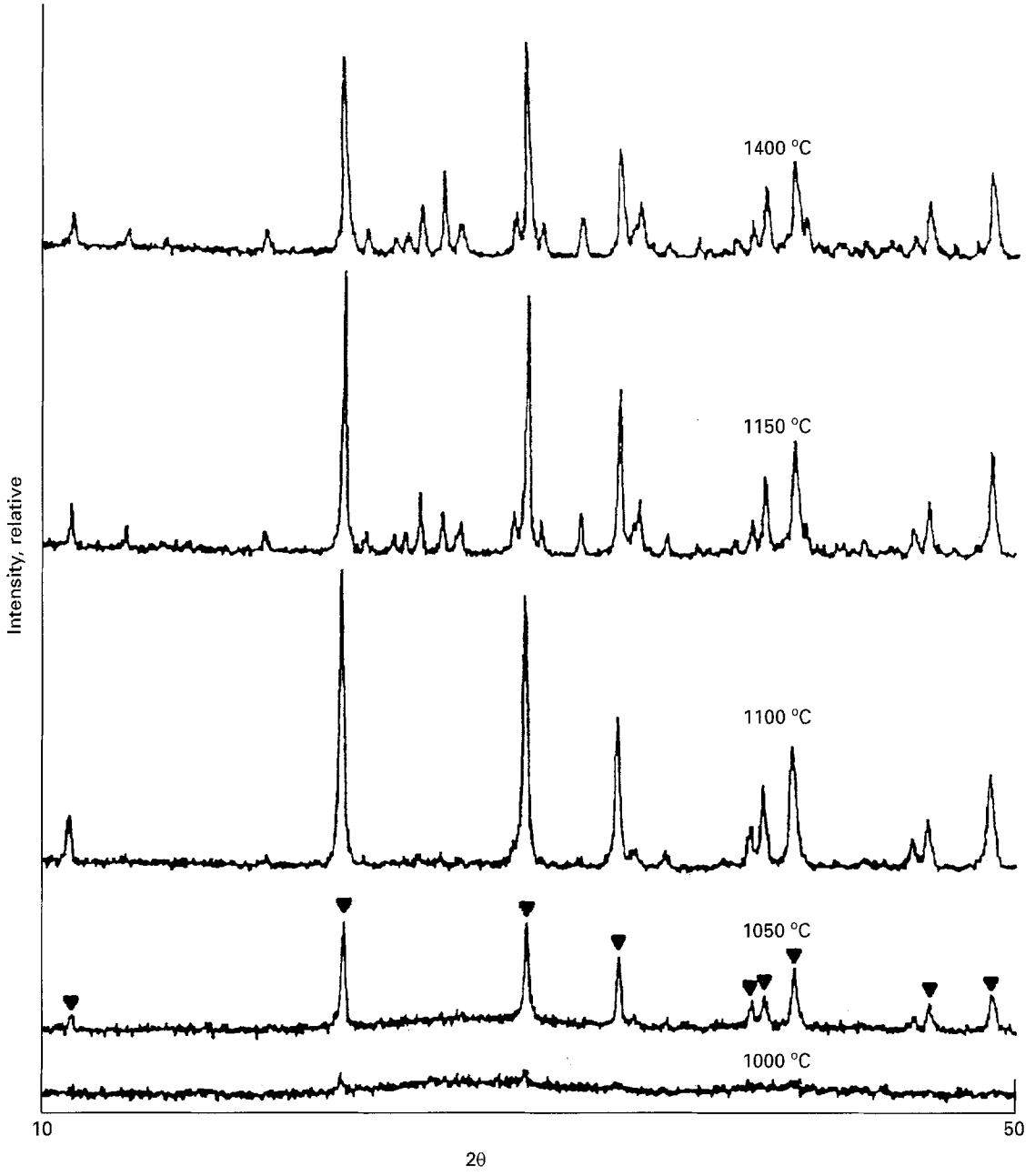

Figure 7 Powder XRD patterns of BAS bulk glass heat treated at various temperatures for 1 h. ▼ BAS hexagonal.

the transformation is not complete even at the highest temperature.

Fig. 8 shows selected powder X-ray diffractograms for bulk BAS glass samples heat treated for 10 h at various temperatures. Initial crystallization of hexacelsian phase is seen at 1000 °C and is complete in the 1050 °C sample. The onset of hexacelsian to monoclinic celsian phase transformation is detected at 1100 °C. The transformation occurs to a greater extent at successively higher temperatures, but is not completed even at 1350 °C.

Fig. 9 shows powder XRD patterns for 1 h heat-treated SAS bulk glass at different temperatures. Initial crystallization of hexacelsian is detected at 1000 °C and is complete in the sample heat-treated at 1100 °C where a trace amount of celsian is also detected. The extent of hexacelsian to celsian transformation increases with temperature. The transformation is complete in the 1250 °C sample where there is complete absence of hexacelsian.

Selected powder XRD patterns for SAS bulk glass samples heat-treated for 10 h at various temperatures are shown in Fig. 10. Crystallization of hexacelsian is detected at 950 °C and is complete in the sample heat-treated at 1000 °C. The hexacelsian to celsian transformation is seen at 1100 °C and celsian is the only phase present in the 1150 °C heat-treated sample.

4.4. Microstructure development

Optical micrographs taken from the polished cross-sections of BAS and SAS bulk glass samples heat treated at various temperatures for 1 or 10 h are shown in Figs 11–14.

The effect of 1 h thermal treatment at four different temperatures on the microstructural development in

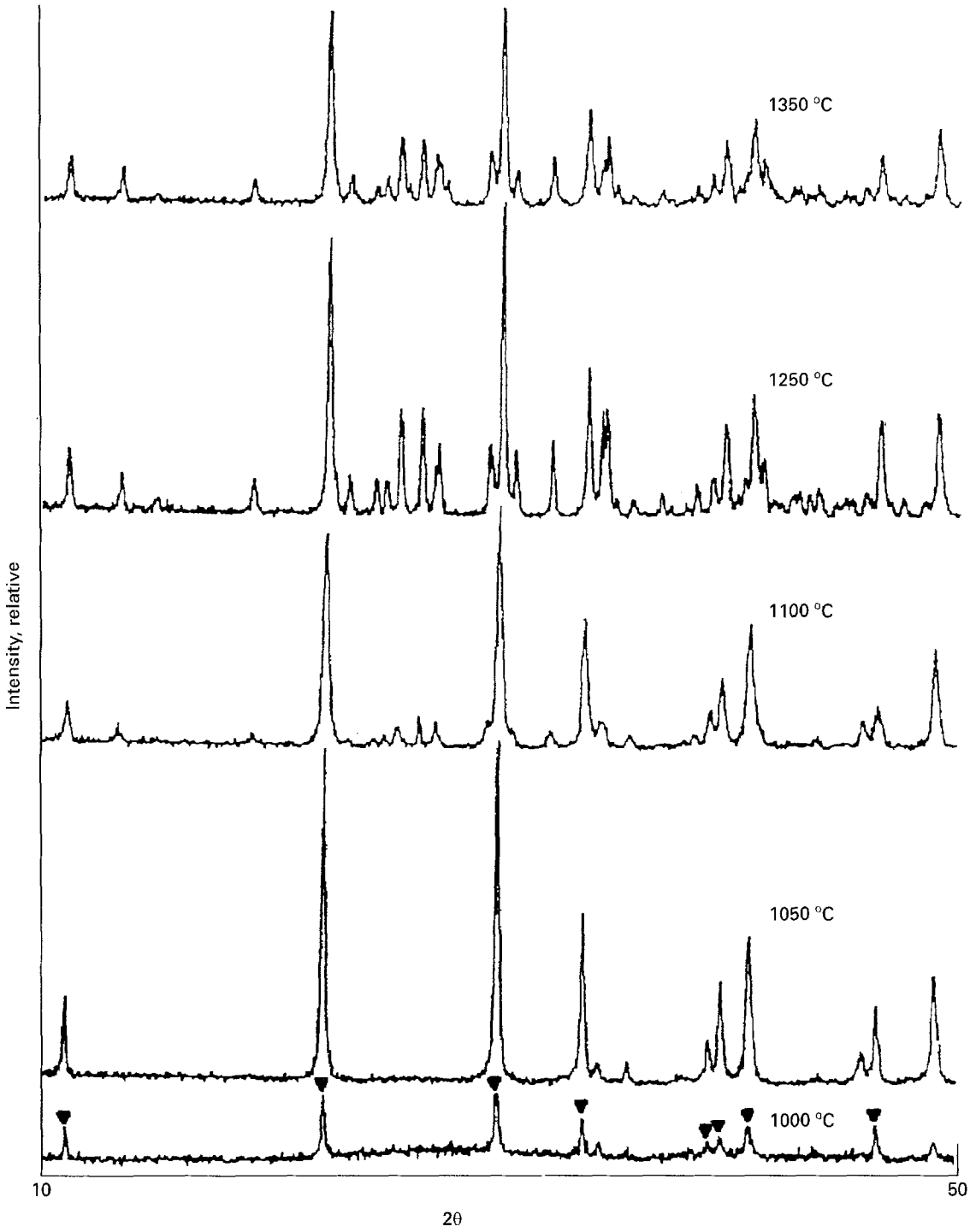

Figure 8 Powder XRD patterns of BAS bulk glass after heat treatments for 10 h at different temperatures. ▼ BAS hexagonal.

BAS glass is presented in Fig. 11. The 1050 °C sample is partially crystallized with the hexacelsian phase nucleating at the surface. The 1100 °C sample has completely crystallized to hexacelsian with a uniform fine grained microstructure. Evidence of grain growth from the sample surface into the bulk is also seen. At 1150 °C, bulk nucleation and transformation to celsian is seen by the appearance of a higher contrast phase within the sample. This is in agreement with previous work in which celsian was not detected by XRD on the surface of a partially crystallized, similar BAS bulk glass [3]. Still further, yet incomplete, transformation to celsian is seen at 1400 °C. Fig. 12 shows the microstructural development in BAS glass samples after 10 h heat treatment at different temperatures. As at 1 h, surface nucleation of hexacelsian is seen, but at 1000 °C due to the longer treatment time. The 1050 °C sample is fully crystallized and large hexacelsian grains have formed from the surface into the bulk of the sample. The 1100 °C sample shows continued grain growth and some of the hexacelsian has begun to transform into fine grained monoclinic celsian in the bulk as seen by the higher contrast celsian grains. Further phase transformation is observed in the 1250 °C sample.

The microstructural development in SAS bulk glass after 1 h isothermal heat treatment at various temperatures is presented in Fig. 13. Surface nucleation of

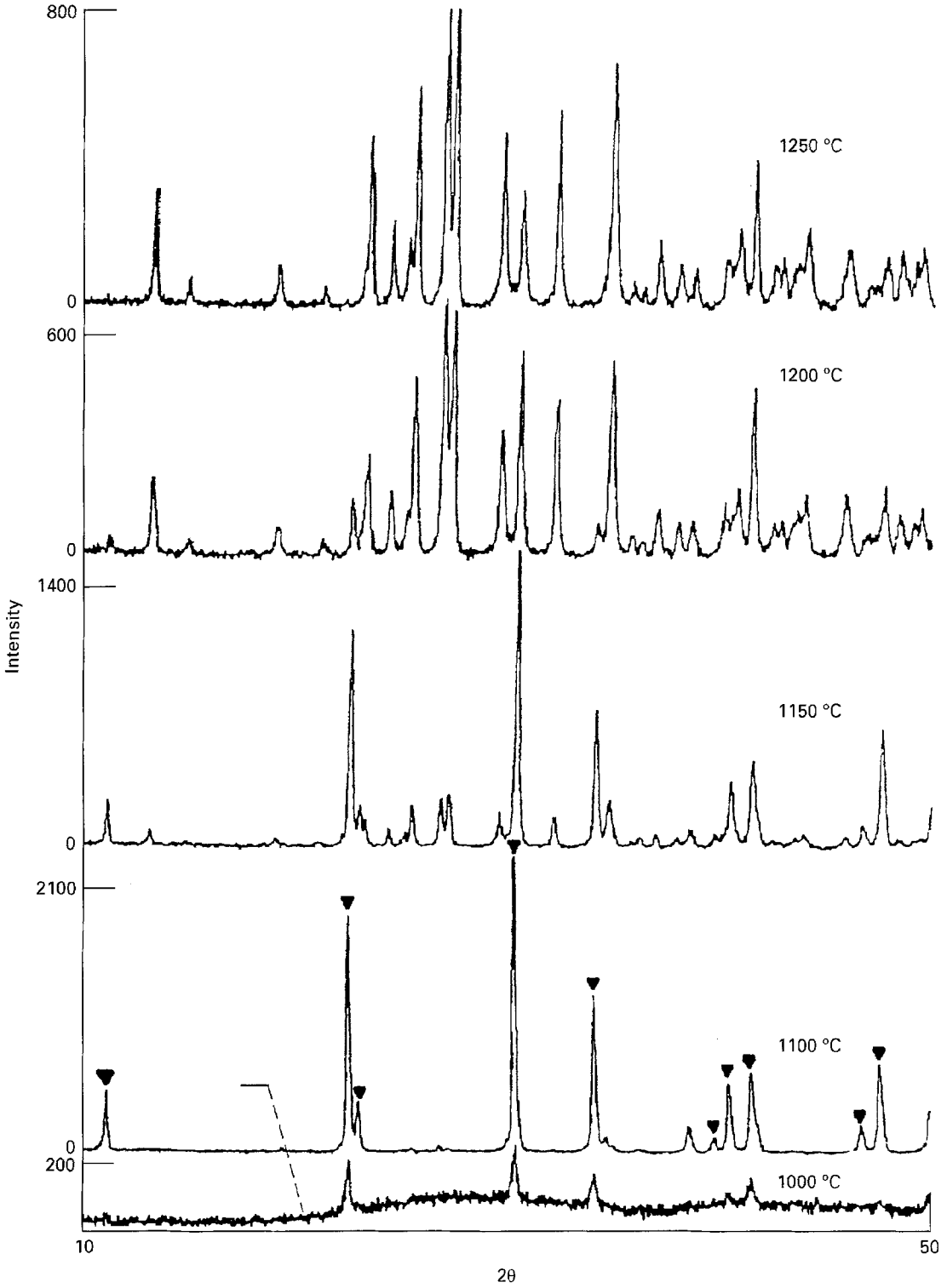

Figure 9 Powder XRD patterns of SAS bulk glass heat treated for 1 h at different temperatures. ▼ SAS hexagonal.

hexacelsian is evident, as in BAS, though this occurs at lower temperatures. Some pullout of hexacelsian is evident in the 1150 °C sample. This is probably due to microcracking resulting from hexacelsian to orthorhombic phase transformation at lower temperature which is accompanied by volume change. In bulk SAS glass, complete transformation to monoclinic celsian is seen at 1250 °C. Fig. 14 shows the microstructures of SAS bulk glass after isothermal heat treatment for 10 h at four different temperatures. As seen previously, surface nucleation and crystallization of hexacelsian occurs at lower temperatures than in BAS. This is followed by bulk nucleation of celsian from the hexacelsian phase. Transformation to celsian is complete in the 1150 °C sample as celsian was the only phase found to be present in this sample from XRD analysis.

The microstructural development in these heat-treated glasses correlates very well with the nucleation and crystal growth of hexacelsian and celsian phases as found from X-ray diffraction analysis results presented above.

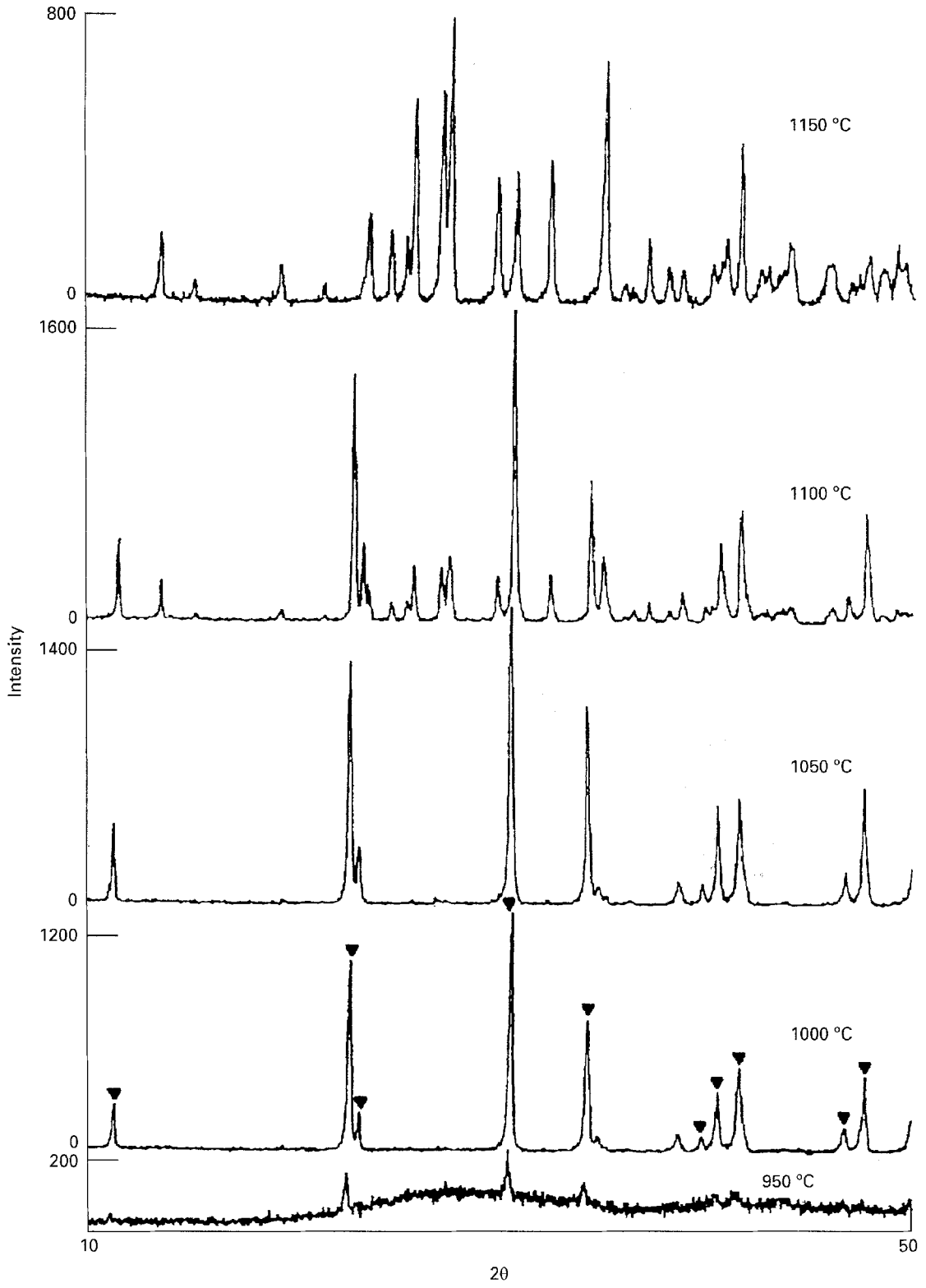

Figure 10 Powder XRD patterns of SAS bulk glass heat treated at various temperatures for 10 h. ▼ SAS hexagonal.

5. Discussion

The crystallization peak maximum in the DSC scans corresponds to the temperature at which the rate of transformation of the viscous liquid into crystals becomes maximum. When the composition of the crystalline phase is different from that of the liquid, the rate of transformation will be controlled by the rate of diffusion through the viscous liquid and the number of crystallization sites to which diffusion can occur. However, when the crystalline phase has the same composition as the liquid, as in the glasses of the present study (see XRD results above), the transformation rate will depend on the density of crystallization sites. If the number of nucleation sites is increased, e.g. by using slower heating rates, the peak maximum will occur at a temperature at which the melt viscosity is higher, i.e. at a lower temperature. This explains the increase in T_p with

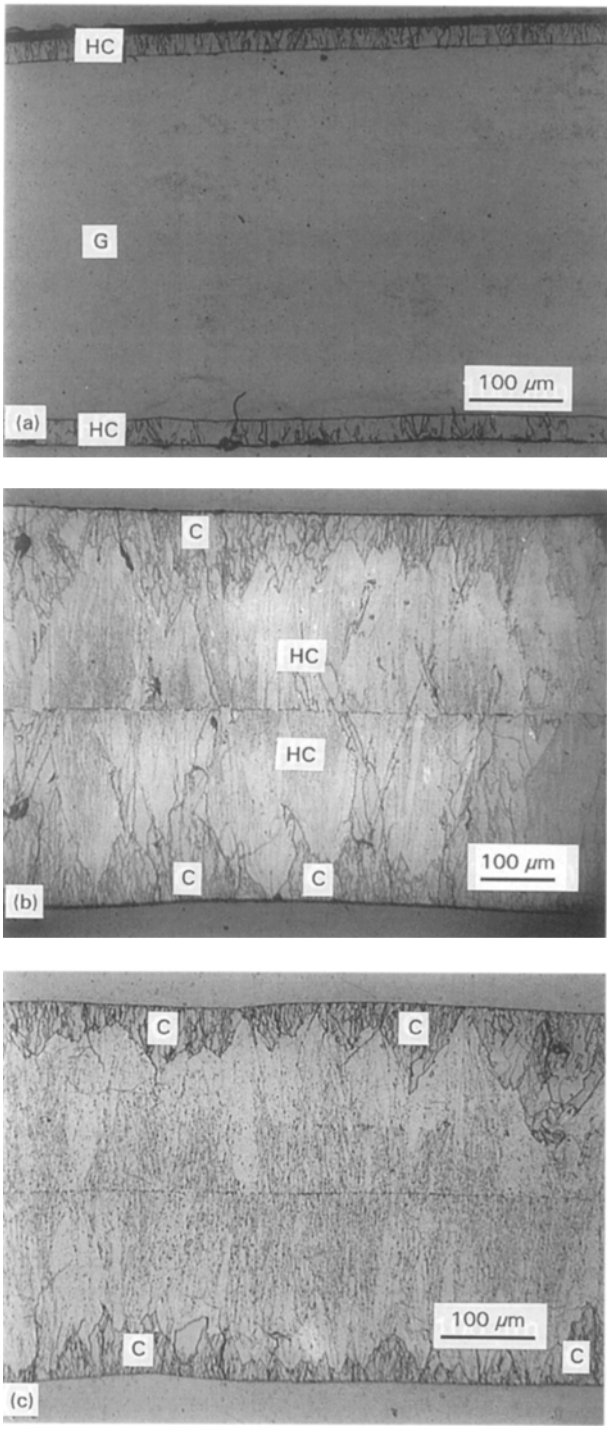

Figure 11 Optical micrographs from polished cross-sections of BAS bulk glass samples heat treated for 1 h at (a) 1050 °C, (b) 1150 °C, and (c) 1400 °C; C celsian, G glass, HC hexacelsian.

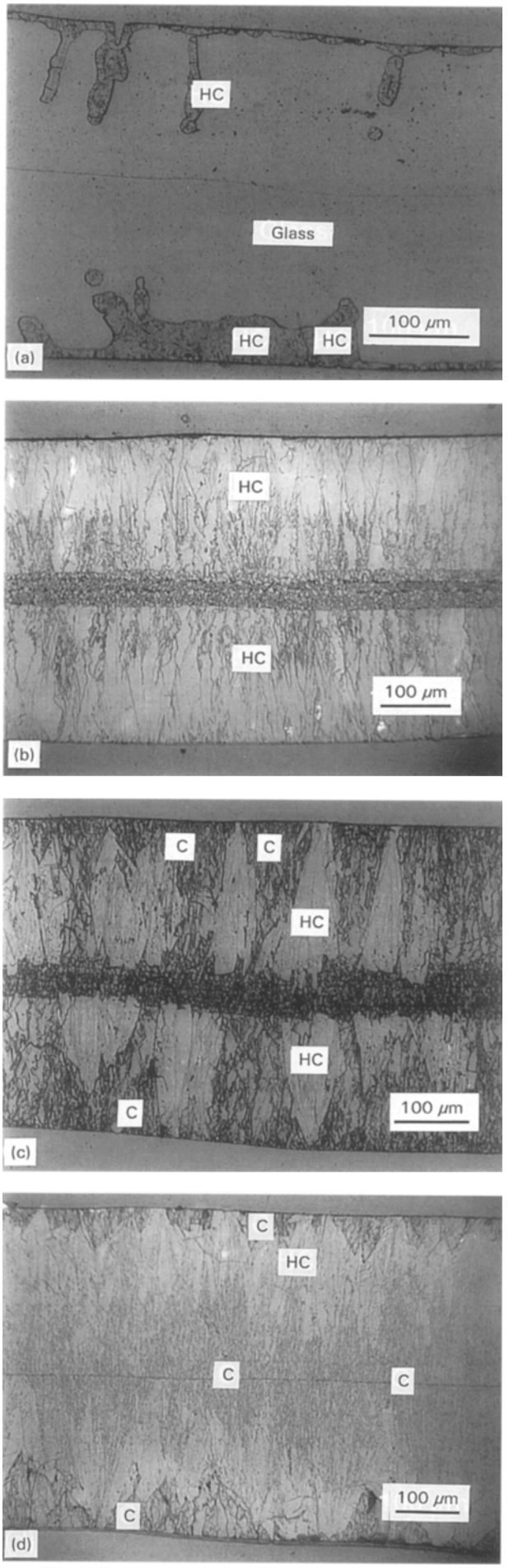

Figure 12 Optical micrographs from polished cross-sections of BAS bulk glass specimens heat-treated for 10 h at (a) 1000 °C, (b) 1050 °C, (c) 1100 °C, and (d) 1250 °C; C celsian, HC hexacelsian.

the scan rate (Tables III and IV) observed in the present study.

On heat treatment, the first phase to crystallize out in both BAS and SAS glasses is the metastable, high-temperature phase hexacelsian rather than the stable, low-temperature form, monoclinic celsian. Formation of metastable crystal phases has also been observed [15, 16] during the devitrification of other glasses. Bahat [4] studied the heterogeneous nucleation of alkaline earth feldspar ($RO–Al_2O_3–SiO_2$ where R = Ba, Sr, or Ca) glasses by a wide variety of nucleating agents. The metastable forms (hexagonal and orthorhombic) of the alkaline earth feldspars nucleated

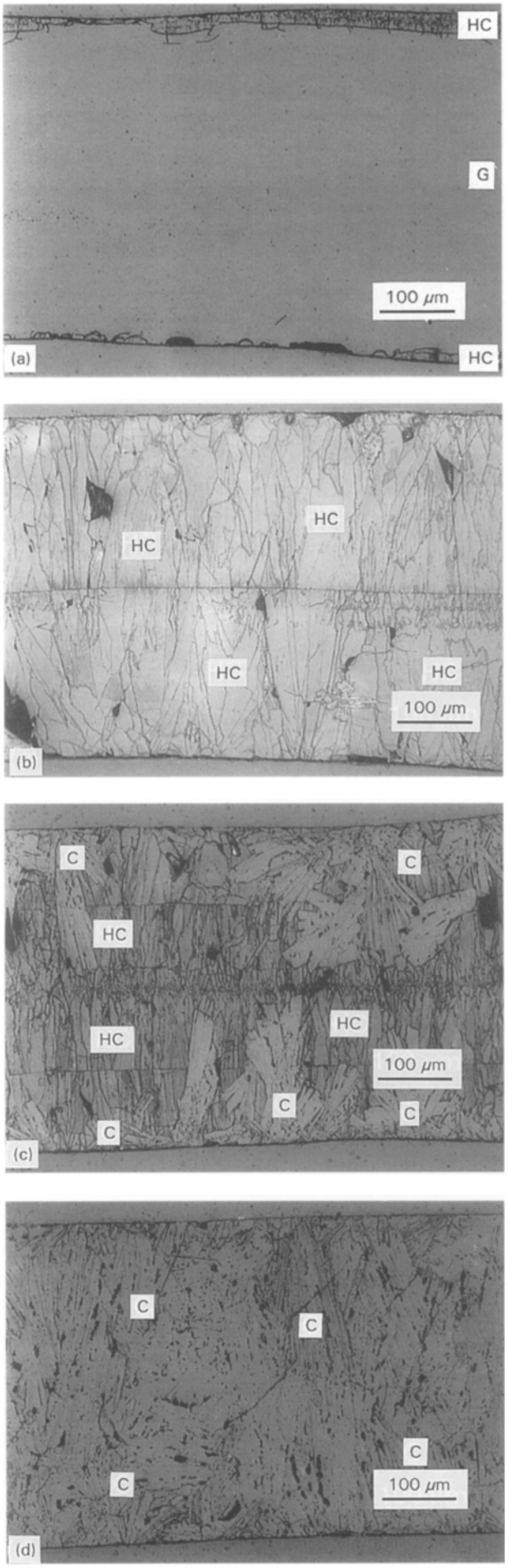

Figure 13 Optical micrographs from polished cross-sections of SAS bulk glass samples heat-treated for 1 h at (a) 1000 °C, (b) 1100 °C, (c) 1150 °C, and (d) 1250 °C; C celsian, G glass, HC hexacelsian.

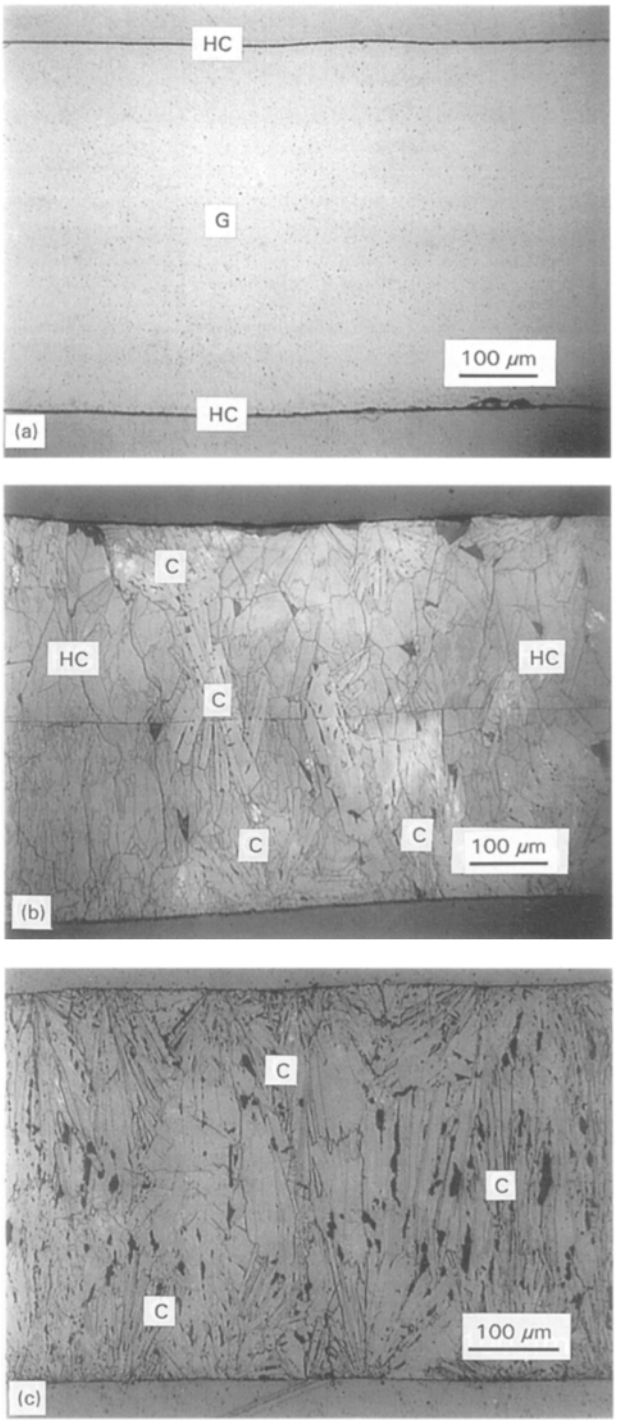

Figure 14 Optical micrographs from polished cross-sections of SAS bulk glass specimens heat-treated for 10 h at (a) 950 °C, (b) 1100 °C, and (c) 1150 °C; C celsian, G glass, HC hexacelsian.

more readily from the glasses than the stable forms (monoclinic and triclinic) due to the simpler structures of the high symmetry modifications. The crystal structure of hexacelsian [5] contains infinite two-dimensional hexagonal sheets consisting of two layers of (Al, Si)O_4 tetrahedra. These tetrahedra share three corners with the remaining apices pointing in the same direction. Two of these sheets share their apical oxygens, forming a double tetrahedral sheet. Ba or Sr ions compensate for the charge difference between Al and Si and occupy positions between the double sheets with 12 equidistant oxygen neighbours. In contrast, monoclinic celsian consists of a three-dimensional

feldspar structure [18] in which all four vertices of the silica tetrahedra are shared, forming a three-dimensional network. As in hexacelsian, Al substitutes for Si so that each Al tetrahedron is surrounded by four predominantly Si tetrahedra and vice versa. Charge compensation is by Ba or Sr ions present in the larger interstices of the framework structure. The Ba or Sr ions have an irregular configuration with 10 oxygen neighbours at several Ba–O or Sr–O distances. Due to these structural differences, the high symmetry hexagonal forms have lower kinetic barriers for nucleation and are the preferred phases to crystallize on heat treatment of BAS and SAS glasses.

The rate of hexacelsian to celsian transformation in $BaAl_2Si_2O_8$ is very sluggish. The solid solubilities [19] of silica in the hexagonal and monoclinic forms of celsian are about 4 and 2 wt %, respectively. During the hexacelsian to celsian transformation, the excess silica must precipitate out. The kinetics of exsolution of silica may be slow and may control the rate of the overall phase transformation. Also, the transformation of hexacelsian to celsian would require the creation of a three-dimensional network from the two-dimensional sheet structure as well as rearrangement of the Ba or Sr sites. This must entail breaking and reforming of the Al–O and Si–O bonds. The single-bond strength of the Si–O bond is 445 kJ mol^{-1} and that of the Al–O bond with an Al co-ordination number of four is 330–423 kJ mol^{-1}. The activation energy for this transformation in the SAS system is reported [7] to be 527 kJ mol^{-1} which is larger than the Si–O and Al–O single bond strengths and is consistent with the mechanism requiring the breaking of the Si–O and Al–O bonds. However, a value of 84 kJ mol^{-1} reported [8] for the similar transformation in BAS is too low and not consistent with the mechanism. Bansal and Drummond [20] recently reanalysed Bahat's data for the BAS system and obtained an activation energy of 373 kJ mol^{-1} for the transformation.

Due to the sluggish [8, 9] kinetics of hexacelsian to celsian transformation in BAS, it is difficult to obtain single phase celsian. In the SAS system [7] however, the rate of this transformation is fast enough to synthesize single phase monoclinic celsian over a wide temperature range.

6. Summary of results

Crystallization kinetics of $BaOAl_2O_32SiO_2$ and $SrOAl_2O_32SiO_2$ glasses in bulk and powder forms have been studied by non-isothermal DSC. Crystallization activation energies have been determined to be 473 and 560 kJ mol^{-1} for BAS glass and 451 and 534 kJ mol^{-1} for SAS glass in bulk and powder forms, respectively. SAS glass crystallized at lower temperature than BAS. Powder glass samples crystallized at lower temperatures than the bulk indicating surface nucleated crystallization. The development of crystalline phases in these glasses as a function of temperature and time of heat treatment has been followed by powder XRD. In both glasses the hexacelsian phase crystallized out first followed by its transformation into monoclinic celsian at higher temperatures. This transformation was very sluggish in BAS but much faster and easier in SAS.

7. Conclusions

Based on the crystallization kinetics and hexacelsian to celsian transformation in BAS and SAS glasses, the SAS glass matrix is preferred over BAS for fibre-reinforced glass–ceramic composites. Lower crystallization temperatures and easier formation of the desired monoclinic celsian phase in SAS would be advantageous during composite processing.

Acknowledgements

Thanks are due to Ralph Garlick for X-ray diffraction measurements.

References

1. N. P. BANSAL, "Ceramic fiber reinforced glass–ceramic matrix composite", U.S. Patent 5,214,004, May 1993.
2. *Idem.*, "Method of producing a ceramic fiber-reinforced glass–ceramic matrix composite," U.S. Patent 5,281,559, Jan. 1994.
3. N. P. BANSAL and M. J. HYATT, *J. Mater. Res.* **4** (1989) 1257.
4. D. BAHAT, *J. Mater. Sci.* **4** (1969) 847.
5. B. YOSHIKI and K. MATSUMOTO, *J. Amer. Ceram. Soc.* **34** (1951) 283.
6. D. BAHAT, *J. Mater. Sci.* **4** (1969) 855.
7. N. P. BANSAL and C. H. DRUMMOND III, *J. Amer. Ceram. Soc.* **76** (1993) 1321.
8. D. BAHAT, *J. Mater. Sci.* **5** (1970) 805.
9. N. P. BANSAL and C. H. DRUMMOND III, unpublished results.
10. W. A. JOHNSON and R. F. MEHL, *Trans. Amer. Inst. Elec. Eng.* **135** (1939) 416.
11. M. AVRAMI, *J. Chem. Phys.* **7** (1939) 1103; **8** (1940) 212; **9** (1941) 177.
12. H. J. BORCHARD, *J. Inorg. Nucl. Chem.* **12** (1960) 252.
13. N. P. BANSAL and R. H. DOREMUS, *J. Thermal Anal.* **29** (1984) 115.
14. N. P. BANSAL, R. H. DOREMUS, A. J. BRUCE and C. T. MOYNIHAN, *J. Amer. Ceram. Soc.* **66** (1983) 223.
15. N. P. BANSAL, A. J. BRUCE, R. H. DOREMUS and C. T. MOYNIHAN, *J. Non-Cryst. Solids* **70** (1985) 379.
16. *Idem., Proc. SPIE* **484** (Society, Photo-Optical Instrument Engineers, Bellingham, WA, 1984) p. 51.
17. G. O. PILOYAN, I. D. RYBACHIKOV and O. S. NOVIKOVA, *Nature* **212** (1966) 1229.
18. R. E. NEWNHAM and H. D. MEGAW, *Acta Crystallogr.* **13** (1960) 303.
19. J. S. MOYA CORRAL and A. GARCIA VERDUCH, *Trans. J. Br. Ceram. Soc.* **77** (1978) 40.
20. N. P. BANSAL and C. H. DRUMMOND III, *J. Mater. Sci. Lett.* **13** (1994) 423.

Received 13 July 1994
and accepted 24 May 1995